Analysis of the effects of macrobend losses in broadband spectrum filtering

2015 Laser Phys. Lett. 12 045103

(http://iopscience.iop.org/1612-202X/12/4/045103)

IOP Publishing | Astro Ltd
Laser Physics Letters
Laser Phys. Lett. **12** (2015) 045103 (6pp)
doi:10.1088/1612-2011/12/4/045103

Analysis of the effects of macrobend losses in broadband spectrum filtering

J C Hernandez-Garcia[1,2], N Jauregui-Vazquez[1], J M Estudillo-Ayala[1], B Ibarra-Escamilla[3], E Vargas-Rodriguez[4], R I Mata-Chavez[4], A D Guzman-Chavez[4] and R Rojas-Laguna[1]

[1] Departamento de Electrónica, Universidad de Guanajuato, División de Ingenierías Campus Irapuato-Salamanca, Carretera Salamanca-Valle de Santiago km 3.5 + 1.8, Comunidad de Palo Blanco, Salamanca, Gto., C.P. 36885, Mexico
[2] Cátedras CONACYT, Consejo Nacional de Ciencia y Tecnología, Dirección Adjunta de Desarrollo Científico, Avenida Insurgentes Sur 1582, Crédito Constructor, Cd. de México, DF, C.P. 03940, Mexico
[3] Departamento de Óptica, Instituto Nacional de Astrofísica, Óptica y Electrónica (INAOE), L. E. Erro 1, Puebla, Puebla, C. P. 72000, Mexico
[4] Departamento de Estudios Multidisciplinarios, Universidad de Guanajuato, División de Ingenierías Campus Irapuato-Salamanca, Av. Universidad s/n, Col. Yacatitas, Yuriria, Gto., C. P. 38940, Mexico

E-mail: rlaguna@ugto.mx

Received 20 January 2015, revised 4 February 2015
Accepted for publication 9 February 2015
Published 25 February 2015

Abstract

In this letter, the effects of bending losses for the development of tunable supercontinuum sources are numerically and experimentally analyzed. Here, the proposed supercontinuum source is based on a very short length segment of standard single-mode fiber (SMF-28) which was used as a nonlinear medium and it was pumped by a microchip Q-switch laser at 1064 nm. In the experimental setup, a section of the optical fiber was wrapped around a mandrel in order to induce bending losses. In addition, by changing the fiber wrapping settings of the SMF-28 the SC source spectrum was filtered at some wavelengths due to mechanical stress. Hence, the source bandwidth can be increased or decreased by selecting the fiber length and by modifying the wrapping settings. Furthermore, in this work it is described as a numerical analysis which helps to support our experimental results. This numerical analysis was based on the fourth-order Runge–Kutta in the interaction picture method and the beam propagation method.

Keywords: supercontinuum generation, fiber optics, nonlinear optics

(Some figures may appear in colour only in the online journal)

1. Introduction

Currently, optical supercontinuum (SC) generation methods have been widely studied with the aim of improving existing sources for applications in telecommunications, spectroscopy, optical metrology and wavelength tunable sources [1–4]. Several authors have presented schemes of SC sources taking advantage of the very fast development of special fibers. For instance, several designs are based on photonic crystal fibers (PCFs) [5–8]. These fibers have large nonlinear coefficients and offer the possibility of shifting their zero dispersion wavelength (ZDW), which is an ideal characteristic for SC generation, achieving spectra ranging from 900–1900 nm under pumping with 1360 nm, 120 fs pulses, in an all-normal dispersion PCF [5], or 350 to over 1700 nm through cascaded PCF tapers pumped with 1064 nm [7]. However, the relatively high cost of PCFs usually limits their use.

Moreover, in the literature some works for SC generation can be found which do not require PCFs in their experimental schemes. Recently, different designs based on dispersion-shifted fibers (DSF) have been presented, which are pumped by a microchip Q-switched laser emitting sub-nanosecond pulses [9]. Other authors have achieved SC

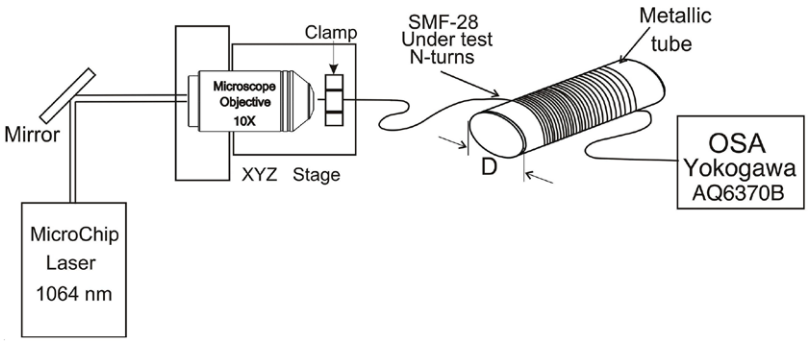

Figure 1. Experimental setup.

sources with a spectral width from 850–2500 nm by using highly nonlinear fiber (HNLF) [10], and a low-noise SC spectrum with controlled intensity distribution over the range 1–2 μm by using hybrid HNLF [11]. Another alternative to SC generation is based on a holmium-doped fiber amplifier, concentrating an average power of 400 mW in the range from 1950–2150 nm [12].

Standard single-mode (SMF) fibers [13], have different advantages such as being relatively inexpensive and they are easy to handle. The design of low-cost SC sources with a simple selectable bandwidth control can be quite important for several scientific and technological applications. For this reason, in this work a SC generation setup based on a SMF-28 fiber pumped with a microchip Q-switched laser at 1064 nm is presented. In this setup, a selectable spectral width was achieved by inducing bending losses in the scheme. Furthermore, the spectral profile of SC source showed notable features as a good spectral flatness. In addition, a numerical analysis is presented that supports the phenomenon that allows the tuning of the SC source, by inducing a filtering effect on the spectrum. Moreover, it is shown that this numerical simulation agrees with the experimental results. Finally, the main advantages of the implemented SC generation technique are the relatively low cost, a good spectral flatness and an easy and flexible bandwidth control.

2. Experimental setup

Recently [14, 15], we have demonstrated the possibility of SC generation by using SMF-28 fiber. Based on these works, we are proposing an experimental arrangement based on mechanical stress (see figure 1). In this setup, different lengths of SMF-28 fiber were tested in order to study the spectral behavior of the SC source. Here, for simplicity, we will only present the results obtained with segments of 30 and 50 m. Moreover, a microchip Q-switched laser operating at 1064 nm, with 9 kHz repetition rate, peak power of 10 kW, pulse energy of 7 μJ and pulses of 700 ps was used as a pump source. The laser beam was coupled into a SMF-28, which was actuated as the nonlinear medium, by using one mirror and a 10 × microscope objective mounted in a *XYZ* stage. In order to induce the tuning effect of the SC source, bending effects were induced by wrapping the SMF-28 in a metallic cylindrical tube with diameter (D). Finally, the spectral response was monitored with an optical spectrum analyzer.

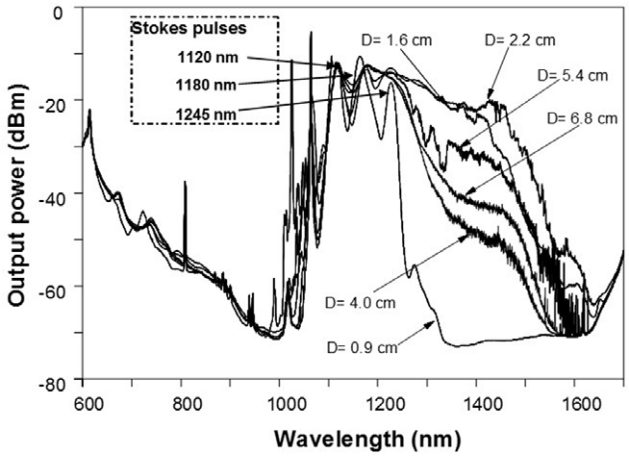

Figure 2. Supercontinuum spectra generated with 30 m of wrapped fiber using different values of bent diameter.

3. Experimental results

For the first case of study, the evolution of the spectral response generated with 30 m of SMF-28 fiber, wrapped around a mandrel with different diameters D, was analyzed. The spectral measurements for this case are shown in figure 2 where it can be appreciated that above the zero dispersion wavelength (ZDW), which for the SMF-28 is ~1313 nm, the SC spectrum is more sensitive to variations of D. For instance, when the SMF-28 fiber was wrapped on a tube with D = 0.9 cm the narrowest SC spectrum, from 1100 to 1250 nm, was generated (see figure 2). For diameters D < 0.9 cm the SC signal was practically attenuated. In contrast, when the fiber was wrapped on a tube with D = 2.2 cm, the most stable and widest spectrum, from 1050–1600 nm, was achieved.

For the second case of study, 50 m of SMF-28 were completely wrapped on a metallic tube with different diameters. For D = 0.9 cm the narrowest SC spectrum was generated, while the most stable SC spectrum was obtained, again, when a D = 2.2 cm was used (see figure 3). Thus, by using these experimental conditions it was possible to obtain a broadband spectrum, from 750 to over 1700 nm, which theoretically is

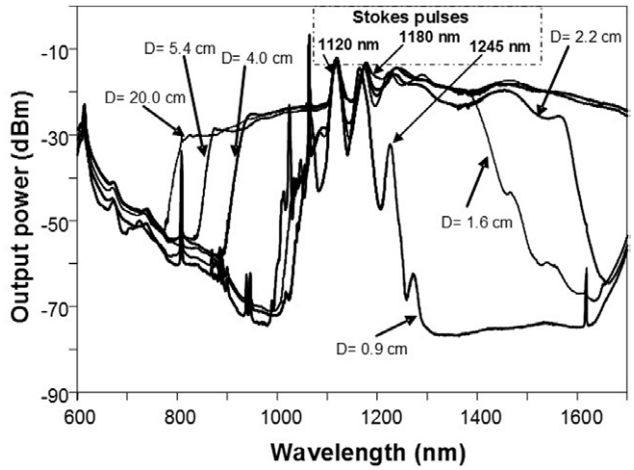

Figure 3. Supercontinuum spectra generated with 50 m of wrapped fiber using different values of bent diameter.

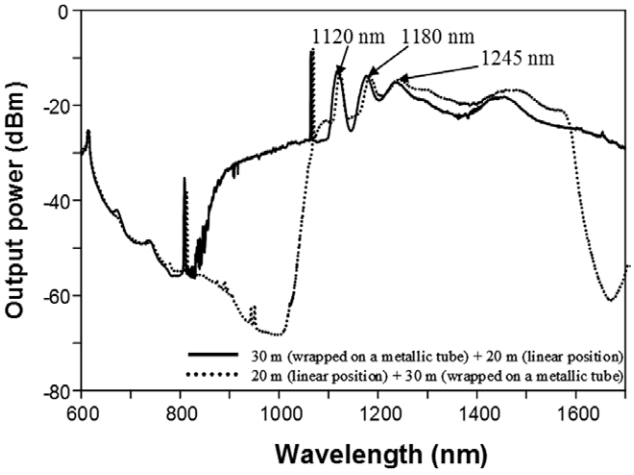

Figure 4. Supercontinuum spectra achieved by modifying the wrapped configuration.

correct, since the interaction with the nonlinear medium is greater than in the previous case. Moreover, when D was 20, 5.4 and 4 cm spectra with wider bandwidths were obtained. However, these presented lower stability than those obtained when a diameter of 2.2 cm was used.

For the third case of study, 50 m of SMF-28 fiber was wrapped in two different configurations: a) the initial 30 m of the fiber were wrapped in the cylindrical tube with a 2.2 cm diameter (which presented the most stable experimental results) while the last 20 m were left unwrapped; b) the initial 20 m of the fiber length were left unwrapped while the last 30 m were wrapped in the cylindrical tube with a 2.2 cm diameter. The experimental results are presented in figure 4, where it can be appreciated that for the first configuration a wider spectrum was achieved, from 800 to over 1700 nm. For the second configuration the obtained SC source has a narrower spectral width, from 1000–1630 nm. Hence, it was demonstrated that by only varying the bending diameter and the wrapping configuration it is possible to control the bandwidth of the proposed SC source.

4. Numerical analysis: fourth-order Runge–Kutta in the interaction picture method and beam propagation method

In order to support the obtained experimental results and to understand the tuning process of the SC source, which was produced by changing the position of the bending mechanism, a numerical analysis was performed. This numerical analysis was based on some works related to the study of wavelength dependence due to bending losses in a SMF-28 fiber [16–20]. In addition, the evolution of nanosecond pulses produced by a microchip laser in a piece of standard fiber under bending effects was analyzed by numerical simulations using the Runge–Kutta in the interaction picture (RK4IP) method [21]. The parameter values used in the numerical analysis correspond to those of the SMF-28 fiber used in our experiment, which are: length of the fiber = 0.05 km (including the wrapped section), fiber dispersion = $-30.17\,\mathrm{ps\,(nm.km)^{-1}}$ and nonlinear coefficient $\gamma = 1.5/\mathrm{W^{-1}\ km^{-1}}$ with a central wavelength of 1064 nm. The value of parameters τ_1, τ_2 and f_r were chosen to provide a good fit to the actual Raman-gain spectrum: $\tau_1 = 12.2$ fs, $\tau_2 = 32$ fs and $f_r = 0.18$, as established in previous studies [22, 23]. The Raman response is described as

$$R(t) = (1 - f_r)\delta(t - \tau_e) + f_r h_R(t), \tag{1}$$

$$h_R(t) = \frac{\tau_1^2 + \tau_2^2}{\tau_1 \tau_2^2} \exp(-t/\tau_2)\sin(t/\tau_1). \tag{2}$$

The RK4IP method uses the general nonlinear Schrödinger equation (GNLSE) given by

$$\frac{\partial A}{\partial z} = -\frac{\alpha}{2}A - \left(\sum_{n\geq 2}\beta_n \frac{i^{n-1}}{n!}\frac{\partial^n}{\partial T^n}\right)A + \mathrm{i}\gamma\left(1 + \frac{1}{\omega_0}\frac{\partial}{\partial T}\right)$$
$$\times\left((1 - f_r)A|A|^2 + f_r A\int_0^\infty h_R(\tau)\,|A(z, T-\tau)|^2\,\mathrm{d}\tau\right), \tag{3}$$

where A is the complex field envelope, z is the distance, and β_n are the dispersion coefficients obtained by a Taylor series expansion of the propagation constant $\beta(\omega)$ around the center frequency (ω_0). In the simulation, we used a value of $\beta_2 = -2.1682\,\mathrm{ps^2\,nm^{-1}}$. This second order dispersion coefficient is sufficient to describe the propagation of the pulse (this was verified numerically by considering higher-order parameters β_n for $n > 2$, showing no significant changes in the spectrum). In the numerical analysis it is important to consider that losses due to the curvature effect (α) are not constant.

Currently, there are several methods which help to predict curvature losses in optical fibers. For optical waveguides with sufficiently large radius of curvature the Marcuse formula is commonly used [17]. This formula agrees well in experiments where the SMF-28 fiber was under bend-induced stress. Bending fiber simulations were performed by using the beam propagation method (BPM), in conjuntion with the conformal mapping technique. The BPM-stimulated bending loss is

a modified method from the original Marcuse formula. The refractive index distribution used in the BPM method [18] is given by

$$\mathrm{n}' = n\left(1 + \frac{x}{R_{\mathrm{eff}}}\right), \tag{4}$$

where $n(x, y)$ is the unperturbed index and R_{eff} is the equivalent bend radius. Note that for silica fiber $R_{\mathrm{eff}}/R \approx 1.28$. By analyzing the BPM method the following relationships are obtained [18],

$$2\alpha = \frac{\pi^{1/2}\kappa^2 \exp\left(-\frac{2\gamma^3 R_{\mathrm{eff}}}{3\beta_z^2}\right)}{2R_{\mathrm{eff}}^{1/2}\gamma^{3/2}V^2 K_{m-1}(\gamma s)k_{m+1}(\gamma s)}, \tag{5}$$

where κ and γ are the normalized propagation constants for the core and the cladding, respectively, V is the normalized frequency, $K_{m\pm1}$ is the modified Bessel function of the second kind. Here, we have that the RK4IP separates the effect of the dispersion ($\hat{D}$) from the nondispersive terms ($\hat{N}$), allowing the use of explicit techniques to simplify the evaluation of the simulation. The choice of a midpoint step, as the separation distance $\mathrm{z}' = z + h/2$, eliminates the exponential dispersion in

$$\hat{N}_1 = \exp(-(z - \mathrm{z}')\hat{D})\hat{N}\exp((z - \mathrm{z}')\hat{D}). \tag{6}$$

In this way the algorithm passes from $A(z, T)$ to $A(z + h, T)$ in a spatial step h, expressed in the normal picture A, which can be written as

$$A_1 = \exp\left(\frac{h}{2}\hat{D}\right)A(z, T), \tag{7}$$

$$k_1 = \exp\left(\frac{h}{2}\hat{D}\right)\left[h\hat{N}(A(z, T))\right]A(z, T), \tag{8}$$

$$k_2 = h\hat{N}(A_1 + k_1/2)[A_1 + k_1/2], \tag{9}$$

$$k_3 = h\hat{N}(A_1 + k_2/2)[A_1 + k_2/2], \tag{10}$$

$$k_4 = h\hat{N}(\exp\left(\frac{h}{2}\hat{D}\right)(A_1 + k_3)) \times \exp\left(\frac{h}{2}\hat{D}\right)[A_1 + k_3], \tag{11}$$

$$A(z + h, T) = \exp\left(\frac{h}{2}\hat{D}\right)[A_1 + k_1/6 + k_2/3 + k_3/3] + k_4/6. \tag{12}$$

The transformation into the normal picture (equation (12)) introduces an overhead evaluation of two FFTs per step; however, this overhead is eliminated by keeping the last trajectory k_4 (equation (11)) in the normal picture. Therefore, each step requires four evaluations of the nonlinear operator ($\hat{N}$) and four evaluations of the exponential dispersion operator $\exp((h/2)\hat{D})$, which requires the computation of eight FFTs [21].

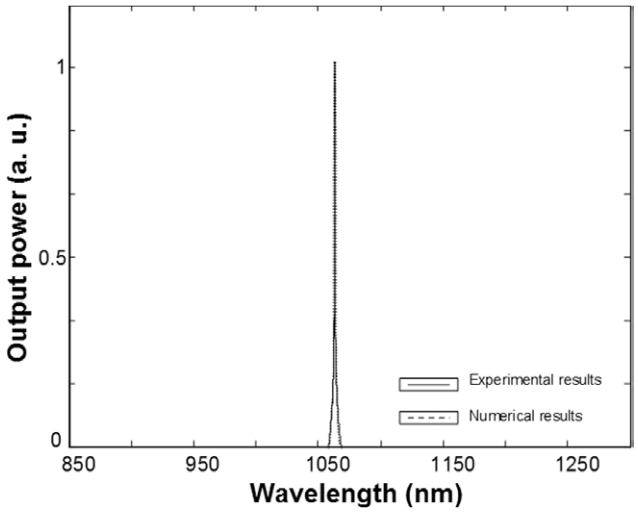

Figure 5. Comparison between numerical and experimental spectra for input signal in the optical fiber scheme.

5. Numerical results

The microchip laser pulse used as the input of the simulation program (based on the RK4IP) was obtained by the description of a generalized Gaussian profile, which can be written as

$$f(x) = a\mathrm{e}^{-\frac{(x-b)^2}{2c^2}}, \tag{13}$$

where a, b, and c are real constants ($a > 0$). The simulated and the experimentally measured input signal are shown in figure 5. For this case, low power was used with the aim of presenting the signal without any nonlinear effect.

In order to observe the bent effects over the final spectrum, based on the experimental configuration, we simulated the curvature in the section of the optical fiber. First, we simulated the case when the first 30 m of SMF-28 fiber were bent with a 2.2 cm diameter while the last 20 m were left in linear position. The simulated spectrum for this wrapping configuration is shown in figure 6, where it can be observed that it presents a plateau with very good flatness within the range from 1120 to above 1700 nm (just on the right side of the pump wavelength). Secondly, we simulated the output spectrum considering that the first 20 m of the SMF-28 fiber were left in linear position while the last 30 m were wrapped considering a 2.2 cm diameter. The simulated spectrum for this configuration is shown in figure 6 where it can be observed that it is attenuated at short and long wavelenghts, obtaining a narrower spectral width from 900 to1650 nm. This configuration allowed us to shorten the bandwidth in comparison with the first case.

The SC source behavior described by the numerical results agrees very well with the experimental results. Therefore, we

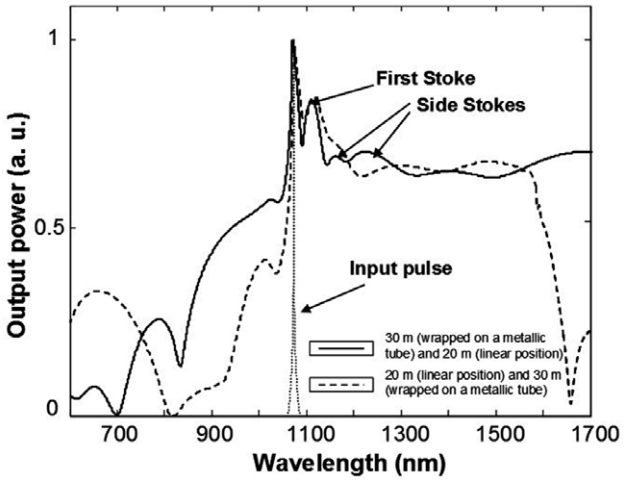

Figure 6. Spectra obtained numerically for different bending configurations.

have that the characteristics of the SC source depend on the properties of the nonlinear medium and the excited nonlinear effects, and the mechanical stresses are supported by the numerical analysis.

6. Principle of operation and discussion

In general, the SC source presented in this work can be explained as the contribution of some nonlinear effects. Here, the three first Stokes pulses, which are located at approximately 1120, 1180 and 1245 nm were observed in all experimental and numerical spectra. This phenomenon is due to the fact that incident light is acting as a pumping source which generates frequency-shifted radiation. In this case, the nonlinear phenomenon is based in the intense pump fields, such that the stimulated Raman scattering, and the Stokes wave shown in figures 2 and 3 grow rapidly inside the medium (in this case SMF-28 fiber) allowing it to achieve a spectral broadening.

The bending losses intensity effects over the n-order Stokes, and over the pump, can be varied depending on the diameter D. This is due to the selection of the effective bend radius which allows the fundamental mode to be relatively stable, while the others exhibited more significant losses [16]. Consequently, it can be expected that self-phase modulation, modulational instability and four-wave mixing should contribute to the SC generation processes [15, 18]. Here, the SC spectral width will be directly affected by bending losses effects which depend on the wavelength [17], and on the bending diameter. In this way, short wavelengths are attenuated due to bending. Moreover, it is important to comment that the SMF-28 will be operating as a multimode fiber since we are pumping with a laser emitting at 1064 nm, and consequently an interaction between some cladding and core modes will be induced. Hence, the contribution of this modal interaction on the SC generation depends on the bending radius (D).

7. Conclusion

This work presented a study on the effect of inducing bending losses in a supercontinuum source. We obtained a relatively simple and low-cost setup for supercontinuum generation. One of the main advantages of the SC source presented here is that it is based on the use of a short piece of standard single-mode fiber as a nonlinear medium. Moreover, the spectral bandwidth of the SC source can be determined by the length of the fiber, the diameter of the mandrel and the proportion of SMF-28 which was wrapped. For instance, when 30 m of SMF-28 were wrapped after 20 m in linear position, it was possible to select the spectral width of the SC within the range from 1050–1600 nm. Similarly, with the opposite fiber configuration it was possible to select the spectral width of the SC source in a range from 800 to above 1700 nm with high flatness. The numerical results are very similar to those obtained in the experimental section. Finally, it is important to mention that this scheme of SC source can have different potential applications due to its low cost and relatively broad spectral range.

Acknowledgments

J C Hernandez-Garcia is supported by CONACYT through chairs for young researchers, project #3155. This work was developed with support in part from CONACYT under Project #183893 and #166361, in part by FOMIX CONACYT-Gobierno del Estado de Guanajuato under project GTO-2012-C02-187434 and in part by CONCYTEG under project 14-PNPC-DPP-Q182-47.

References

[1] Tamura K, Kubota H and Nakazawa M 2000 *IEEE J. Quantum Electron.* **36** 773
[2] Fedotov A B, Zheltikov A M, Ivanov A A, Alfimov M V, Chorvat D, Chorvat D, Beloglazov V I, Melnikov L A, Skibina N B, Tarasevitch A P and Von der Linde D 2000 *Laser Phys.* **10** 723
[3] Wang Y M, Zhao Y H, Nelson J S, Chen Z P and Windeler R S 2003 *Opt. Lett.* **28** 182
[4] Levick A P, Greenwell C L, Ireland J, Woolliams E R, Goodman T M, Bialek A and Fox N P 2014 *Appl. Opt.* **53** 3508
[5] Stepniewski G, Klimczak M, Bookey H, Siwicki B, Pysz D, Stepien R, Kar A K, Waddie A J, Taghizadeh M R and Buczynski R 2014 *Laser Phys. Lett.* **11** 055103
[6] Hernandez-Garcia J C, Estudillo-Ayala J M, Mata-Chavez R I, Pottiez O, Rojas-Laguna R and Alvarado-Mendez E 2013 *Laser Phys. Lett.* **10** 075101
[7] Chen H H, Chen Z L, Zhou X F and Hou J 2013 *Laser Phys. Lett.* **10** 085401
[8] Dvoyrin V V and Sorokina I T 2014 *Laser Phys. Lett.* **11** 085108
[9] Mussot A, Sylvestre T, Provino L and Maillotte H 2003 *Opt. Lett.* **28** 1820
[10] Nicholson J W, Abeeluck A K, Headley C, Yan M F and Jorgensen C G 2003 *Appl. Phys.* B **77** 211

[11] Korel I I, Nyushkov, Denisov V I, Pivtsov V S, Koliada N A, Sysoliatin A A, Ignatovich S M, Kvashnin N L, Skvortsov M N and Bagayev S N 2014 *Laser Phys.* **24** 074012
[12] Kamynin V A, Volkov I A, Nishchev K N, Paramonov V M and Kurkov A S 2014 *Laser Phys. Lett.* **11** 055105
[13] Courvoisier C, Mussot A, Bendoula R, Sylvestre T, Reyes J G, Tribillon G, Wacogne B, Gharbi T and Maillotte H 2004 *Laser Phys.* **14** 507
[14] Hernandez-Garcia J C, Pottiez O and Estudillo-Ayala J M 2012 *Laser Phys.* **22** 221
[15] Hernandez-Garcia J C, Estudillo-Ayala J M, Pottiez O, Rojas-Laguna R, Mata-Chavez R I and Gonzalez-Garcia A 2012 *Opt. Commun.* **292** 126
[16] Wang Q, Rajan G, Wang P and Farrell G 2007 *Opt. Express* **15** 4909
[17] Marcuse D 1976 *J. Opt. Soc. Am.* **66** 216
[18] Schermer R T and Cole J H 2007 *IEEE J. Quantum Electron.* **43** 899
[19] Kuzin E A, Beltran-Perez G, Basurto-Pensado M A, Rojas-Laguna R, Andrade-Lucio J A, Torres-Cisneros M and Alvarado-Mendez E 1999 *Opt. Commun.* **169** 87
[20] Sharma A B, Ai-Ani A H and Halme S J 1984 *Appl. Opt.* **23** 3297
[21] Hult J 2007 *J. Lightwave Technol.* **25** 3770
[22] Blow K J and Wood D 1989 *J. Quantum Electron.* **25** 2665
[23] Stolen R H, Gordon J P, Tomlinson W J and Haus H A 1989 *J. Opt. Soc. Am.* B **6** 1159